

Magnetic properties of diluted magnetic semiconductors: Quantum Monte Carlo approach

Jun-ichiro Ohe^{a,*}, Yoshihiro Tomoda^a, Nejat Bulut^a, Ryotaro Arita^b, Kazuma Nakamura^b, Sadamichi Maekawa^a

^a Institute for Materials Research, Tohoku University, Sendai 980-8577, Japan

^b Department of Applied Physics, University of Tokyo, Bunkyo-ku, Tokyo 113-8561, Japan

ARTICLE INFO

Available online 17 June 2009

Keywords:

Dilute magnetic semiconductor
Magnetic impurity
Quantum Monte Carlo method

ABSTRACT

The magnetic correlation between magnetic impurities in semiconductors is investigated by performing the quantum Monte Carlo (QMC) simulation. The Anderson Hamiltonian with the realistic parameters obtained by the local density approximation (LDA) calculation is employed. The LDA calculation gives a dispersion of the host (GaAs) electron and the mixing energy between host and magnetic impurity (Mn). The mixing between host and impurity electrons generates the impurity bound state in the energy gap of semiconductors. The long range ferromagnetic coupling is observed when the Fermi energy locates between the band edge and the impurity bound state. The ferromagnetic coupling is enhanced by decreasing temperature.

© 2009 Elsevier B.V. All rights reserved.

1. Introduction

The ferromagnetism in III–V semiconductors with the transition metal doping, called as diluted magnetic semiconductors (DMSs), has attracted much attention from the field of semiconductor-based spin-electronics (spintronics) [1–3]. It has been shown experimentally that the Curie temperature T_C and the coercive field H_c are varied by changing the hole density [4,5]. However, the origin of ferromagnetic coupling in DMSs remains controversial because of its complex features [6]. In DMSs, such as (Ga,Mn)As, both carriers and magnetization are provided by Mn ions. The hybridization between extended electrons of GaAs host and localized electrons of Mn induces the impurity band (IB). Optical measurements suggested that the IB is generated in the semiconductor gap, and the chemical potential is located around IB [7,8]. It is natural to consider the holes and IB play a crucial role for the ferromagnetic coupling. By theoretical works, the ferromagnetic coupling is observed within the Hartree Fock approximation. However, it is pointed out that such a mean field theory is not enough to estimate actual T_C [9]. It is also pointed out that the band structure and the mixing energy affects the magnetic properties in semiconductors host. To investigate the magnetic properties in DMSs precisely, one needs to treat the Coulomb interaction free from the mean field approximation and use the realistic band structure and the mixing energy. To design the high T_C DMSs, a theoretical investigation of magnetism for finite temperatures is required.

In this report, we investigate the magnetism of (Ga,Mn)As at finite temperatures with the actual band structure and the hybridization energy. The impurity Anderson Hamiltonian [10] is used to calculate the magnetic properties. In order to describe the material parameters of (Ga,Mn)As, we calculate the band structure and the hybridization energy by using the density functional theory (DFT) formulated in terms of maximally localized Wannier functions (MLWFs) [11]. We employ the Quantum Monte Carlo (QMC) technique for calculating the magnetic properties of both localized Mn electrons and extended GaAs electrons. Results show that the impurity bound state (IBS) is generated around 0.1 eV above the top of the valence band. When the chemical potential is located between IBS and the valence band, we obtain the ferromagnetic coupling between two impurities and it is enhanced by decreasing temperatures. The origin of the ferromagnetic coupling is due to the anti-ferromagnetic coupling between the impurity and carriers. Achievements of quantitative analysis with actual material parameters suggests that the model and method employed in the present work is a powerful tool for investigating and designing the high T_C DMSs.

2. Model and method

The diluted magnetic semiconductors can be modeled by the impurity Anderson Hamiltonian [10],

$$H = \sum_{\alpha, \mathbf{k}, \sigma} (\varepsilon_{\alpha \mathbf{k}} - \mu) n_{\alpha \mathbf{k} \sigma} + \sum_{\xi, i, \sigma} (\varepsilon_d - \mu) n_{\xi i \sigma} + \sum_{\alpha, \mathbf{k}, \xi, i, \sigma} (V_{\alpha \mathbf{k}, \xi i} c_{\alpha \mathbf{k} \sigma}^\dagger d_{\xi i \sigma} + h.c.) + U \sum_{\xi, i} n_{\xi i \uparrow} n_{\xi i \downarrow}, \quad (1)$$

* Corresponding author.

E-mail address: johe@imr.tohoku.ac.jp (J.-i. Ohe).

where $c_{\mathbf{k}\sigma}^\dagger$ ($c_{\mathbf{k}\sigma}$) is a creation (annihilation) operator of a host electron (GaAs) with wave vector \mathbf{k} and spin σ in the band α . $d_{\xi i\sigma}^\dagger$ is the creation operator for a localized electron of the orbital ξ at an impurity (Mn) site i . The number operators of electron are $n_{\mathbf{k}\sigma} = c_{\mathbf{k}\sigma}^\dagger c_{\mathbf{k}\sigma}$, $n_{\xi i\sigma} = d_{\xi i\sigma}^\dagger d_{\xi i\sigma}$. $\varepsilon_{\mathbf{k}}$ is the energy of host electrons, ε_d is the bare energy of localized electrons, μ is the chemical potential. $V_{\mathbf{k},\xi i}$ is the mixing energy between the host electrons and the localized electrons, and U is the Coulomb energy of localized electrons at the impurity sites. The mixing energy $V_{\mathbf{k},\xi i}$ at impurity site \mathbf{r}_i is calculated by Bloch functions of host electrons $\psi_{\mathbf{k}\sigma}(\mathbf{r})$ and localized orbital functions $\varphi_{\xi i}(\mathbf{r})$,

$$V_{\mathbf{k},\xi i} = \int d\mathbf{r} \psi_{\mathbf{k}\sigma}(\mathbf{r})^* H \varphi_{\xi i}(\mathbf{r}) = V_{\mathbf{k},\xi} e^{-i\mathbf{k}\cdot\mathbf{r}_i}, \quad (2)$$

where the Bloch function is expressed as $\psi_{\mathbf{k}\sigma}(\mathbf{r}) = f_{\mathbf{k}\sigma}(\mathbf{r}) e^{i\mathbf{k}\cdot\mathbf{r}}$ with a periodic function $f_{\mathbf{k}\sigma}(\mathbf{r})$. In order to construct a realistic model for (Ga,Mn)As, we first perform an electronic structure calculation using the local density approximation (LDA) within the density functional theory. We take a supercell which contains $3 \times 3 \times 3$ primitive cells of GaAs, and replace one of Ga with Mn. Then we make the maximally localized Wannier functions [11] using the Bloch functions within the energy window $-7 \text{ eV} < \varepsilon_k - E_F < 10 \text{ eV}$, where ε_k is the eigenenergy of the Bloch states and E_F is the Fermi energy. The MLWFs centered at Ga and As atoms have an sp^3 character, while the MLWFs located at Mn atoms have five d-orbital symmetries. Then we represent the LDA Hamiltonian in terms of the MLWFs. The size of the resulting effective Hamiltonian is 217×217 , where it should be noted that we have four sp^3 -orbitals for each Ga and As and five 3d-orbitals for Mn, and there are 53 Ga and As atoms and one Mn in the unit cell. This model describes the conduction bands of GaAs as well as the valence bands as shown in Fig. 1(a). The origin of the energy is set to the top of valence band. We consider eight bands originating from the sp^3 -orbitals at Ga and As sites. The mixing energies $V_{\mathbf{k},\xi i}$ are calculated by taking into account all hopping integrals between Wannier orbitals in $5 \times 5 \times 5$ supercells. Fig. 1(b) shows the mixing energy between the electrons in the valence band and impurity states. Each supercell consists of an MnAs and eight GaAs primitive cell. We perform the Monte Carlo simulation for the one- and two-impurity models by using the results of *ab initio* technique. The bare energy of localized state ε_d is fixed to -2.0 eV . We also fix the Coulomb energy to $U = 4.0 \text{ eV}$ [12].

When an Mn ion is substituted with Ga, the five d-orbitals of the Mn ion are split into the threefold t_{2g} -orbitals and the twofold e_g -orbitals by the tetrahedral crystal field. Since e_g -orbitals has a

low energy compared with the chemical potential, e_g -orbitals are neglected. The Hund coupling is not included in the present work. Therefore, three t_{2g} -orbitals are equivalent for the magnetic properties.

The magnetic correlation function between localized electrons are defined as

$$\begin{aligned} \langle M_{\xi i} M_{\xi j} \rangle &= \sum_{\sigma, \sigma'} \sigma \sigma' \langle n_{\xi i\sigma} n_{\xi j\sigma'} \rangle \\ &= \sum_{\sigma, \sigma'} \sigma \sigma' [g_{dd}^\sigma(0; \xi i, \xi i) g_{dd}^{\sigma'}(0; \xi j, \xi j) \\ &\quad - \delta_{\sigma\sigma'} g_{dd}^\sigma(0; \xi i, \xi j) g_{dd}^\sigma(0; \xi j, \xi i)], \end{aligned} \quad (3)$$

where the magnetization operator is $M_{\xi i} = \sum_{\sigma=\pm 1} \sigma n_{\xi i\sigma}$. Eq. (3) indicates the square of magnetic moment $\langle (M^z)^2 \rangle$ at orbital ξ at site i for $i = j$, while it indicates the magnetic correlation between two impurities, $\langle M_i^z M_j^z \rangle$, for $i \neq j$. The Matsubara Green's function is

$$g_{dd}^\sigma(\tau; \xi i, \xi j) = -\langle T_\tau d_{\xi i\sigma}(\tau) d_{\xi j\sigma}^\dagger \rangle, \quad (4)$$

where T_τ is the Matsubara time-ordering operator. Similarly, we define the magnetic correlation between an impurity and host electrons at site \mathbf{r} ,

$$\langle M^z m^z \rangle = \sum_{\sigma, \sigma', \alpha} \sigma \sigma' \langle n_{\xi i\sigma} n_{\mathbf{r}\sigma'} \rangle, \quad (5)$$

where the Green's function is defined as the same manner with Eq. (4). The annihilation operator of host electrons at site \mathbf{r} is given by $c_{\mathbf{r}\sigma} = (1/\sqrt{N}) \sum_{\mathbf{k}} e^{-i\mathbf{k}\cdot\mathbf{r}} c_{\mathbf{k}\sigma}$ where N is the number of the lattice. We use the Hirsch-Fye technique for calculating one- and two-impurity cases [13,14]. In this calculation, the chemical potential is considered as a parameter, while it should be determined by the number of impurities. Obtained results in this letter corresponding to the low-doped regime of (Ga,Mn)As [15].

3. Results and discussions

Inset of Fig. 2 shows the square of the impurity magnetic moment as a function of the chemical potential μ at various temperatures T . In this calculation, we use the single-impurity Anderson model, and results are the average of three degenerate t_{2g} -orbitals. The $(M^z)^2$ close to unity when the impurity orbital is partially occupied. For the high temperature ($T = 730 \text{ K}$), the $(M^z)^2$ gradually increases due to the temperature smearing of the electron population. By decreasing temperature, it shows step-like behavior around $\mu \sim 0.1 \text{ eV}$. This indicates that the IBS is located around 0.1 eV . Experimentally, the angle-resolved photoemission spectroscopy (ARPES) observed an impurity-induced band that is located near the Fermi level [8]. The infrared optical absorption [7] also showed that the chemical potential resides in impurity-induced states above the top of the valence band. Therefore, the calculated IBS well describes the IB obtained by these experiments.

Fig. 2 shows an impurity-impurity magnetic correlation $\langle M_i^z M_j^z \rangle$ in a GaAs host for the two-impurity Anderson model. The distance between impurities is defined as $|\mathbf{r}|/a$, where $a = 5.69 \text{ \AA}$ is the lattice constant of GaAs. The chemical potential is fixed to $\mu = 0.05 \text{ eV}$ that locates near the IBS [7,8]. From this figure, we observe the ferromagnetic coupling that reaches to the 4th neighbor site. It is also clear that the ferromagnetic coupling is enhanced by decreasing temperature.

The origin of the ferromagnetism is clarified by observing the magnetic correlation between carriers and impurities. By doping Mn in GaAs, an Mn provides a hole carrier. The hybridization between the d-states of doped impurity and the sp^3 -states of a host semiconductor generates the spatially extended p-hole states

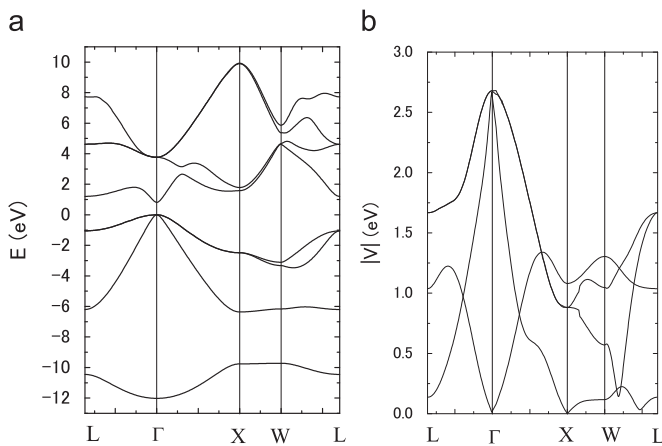


Fig. 1. (a) Calculated band structures of the GaAs. Four conduction bands and four valence bands are shown. (b) The mixing energy between electrons in valence band and the impurity state.

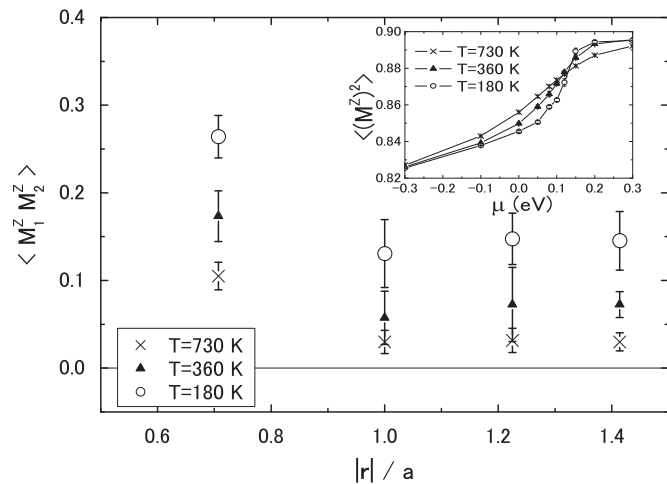


Fig. 2. Magnetic correlation between two impurities at various temperatures. The chemical potential is fixed to 0.05 eV. $a = 5.69 \text{ \AA}$ is the lattice constant of GaAs. Inset shows the square of the magnetic moment in the impurity state.

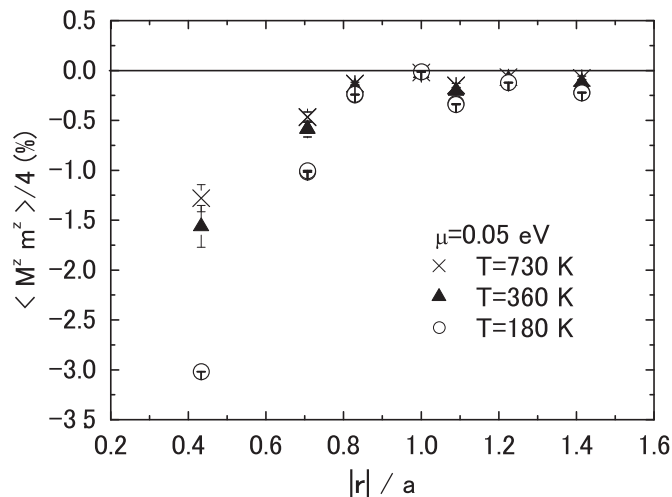


Fig. 3. Magnetic correlation between carriers and the impurity state. Other parameters are the same as those in Fig. 2.

in the valence band. Simultaneously, the hybridization induces the IBS which is split-off from the valence band as shown in Fig. 1. Fig. 3 shows the impurity–host magnetic correlation as a function of $|r|/a$ at various T . The anti-ferromagnetic coupling is observed and it is enhanced by decreasing temperature. When another impurity exists in the host–impurity anti-ferromagnetic coupling regime, these two impurities show ferromagnetic coupling.

4. Summary

In summary, we have investigated the magnetic properties of transition metal doped in the semiconductors host. We used the impurity Anderson Hamiltonian for describing the (Ga,Mn)As. The parameters appearing in the Hamiltonian are calculated from the density functional theory with the maximally localized Wannier functions. Obtained parameters well describes the band structure of GaAs and the mixing energy between the host and the impurity state. For calculating the magnetic properties, the Quantum Monte Carlo technique free from the mean field approximations is employed with the Hirsch–Fye algorithm. The hybridization between impurity and host electrons generates the impurity bound state above the valence band. We observed the ferromagnetic coupling between two Mn impurities when the chemical potential is located around the IBS. The ferromagnetic coupling is enhanced by decreasing temperature. The microscopic origin of ferromagnetic coupling between magnetic impurities is described by double resonance coupling that is originating from the anti-ferromagnetic coupling between host and impurity state. We note that these calculations are easily applied to other host semiconductors and impurities.

Acknowledgments

The authors are grateful to H. Ohno and M.E. Flatté for valuable discussions. This work was supported by the NAREGI Nanoscience Project and a Grand-in Aid for Scientific Research from the Ministry of Education, Culture, Sports Science and Technology of Japan.

References

- [1] S. Maekawa (Eds.), Concepts in Spin Electronics, Oxford University Press, Oxford, 2006.
- [2] I. Žutić, J. Fabian, S. Das Sarma, Rev. Mod. Phys. 76 (2004) 323.
- [3] T. Jungwirth, J. Sinova, J. Mašek, J. Kučera, A.H. MacDonald, Rev. Mod. Phys. 78 (2006) 809.
- [4] H. Ohno, D. Chiba, F. Matsukura, T. Omiya, E. Abc, T. Dietl, Y. Ohno, K. Ohtani, Nature 408 (2000) 944.
- [5] D. Chiba, M. Yamanouchi, F. Matsukura, H. Ohno, Science 301 (2003) 943.
- [6] T. Dietl, J. Phys. Condens. Matter 19 (2007) 165204.
- [7] K.S. Burch, D.B. Shrekenhamer, E.J. Singley, J. Stephens, B.L. Sheu, R.K. Kawakami, P. Schiffer, N. Samarth, D.D. Awschalom, D.N. Basov, Phys. Rev. Lett. 97 (2006) 087208.
- [8] J. Okabayashi, A. Kimura, O. Rader, T. Mizokawa, A. Fujimori, T. Hayashi, M. Tanaka, Phys. Rev. B 64 (2001) 125304.
- [9] N. Bulut, K. Tanikawa, S. Takahashi, S. Maekawa, Phys. Rev. B 76 (2007) 045220.
- [10] F.D.M. Haldane, P.W. Anderson, Phys. Rev. B 13 (1976) 2553.
- [11] N. Marzari, D. Vanderbilt, Phys. Rev. B 56 (1997) 12847.
- [12] J. Okabayashi, A. Kimura, O. Rader, T. Mizokawa, A. Fujimori, T. Hayashi, M. Tanaka, Phys. Rev. B 58 (1998) R4211.
- [13] J.E. Hirsch, R.M. Fye, Phys. Rev. Lett. 56 (1986) 2521.
- [14] R.M. Fye, J.E. Hirsch, D.J. Scalapino, Phys. Rev. B 35 (1987) 4901.
- [15] T. Jungwirth, et al., Phys. Rev. B 76 (2007) 125206.